

Design and analysis of three phase inverter based Solar PV powered single switch Buck-Boost converter with reduced THD for industrial applications

Case Study

Maheshwari L.

Vels Institute of Science Technology and Advanced Studies,
Chennai, Tamilnadu, India
saimahi.eee@gmail.com

Premila T. R.

Vels Institute of Science Technology and Advanced Studies,
Chennai, Tamilnadu, India
trpremilashaji@gmail.com

Abstract – In recent times development of economical & feasible eco-friendly renewable source powered power electronic converters have become more attractive in multiple areas such as automotive, house appliances and industrial applications etc., Bucking and boosting of voltage according to the requirement is also much needed. So, this work proposes a solar photovoltaic (SPV) powered single switch buck-boost converter for industrial applications which reduces implementation cost, minimal voltage and current stress across the capacitors and diodes and less switching power losses. The work structure comprises of solar PV source with modified perturbation and observation (P&O) algorithm based maximum power point tracker (MPPT), single switch buck-boost dc-dc converter, battery backup to store excess energy, three phase inverter with sinusoidal pulse width modulation (PWM) to find optimal switching angles for harmonic control and 3 phase (Φ) induction motor load. Along with the proposed single switch buck-boost converter, an EMI input filter is included to investigate the harmonic reduction. It also uses the Fast Fourier Transform (FFT) analysis with the reduction of supply voltage harmonics generated by the 3 Φ induction motor drive. The DC link is connected with the VSI (voltage source inverter) and then it is converted to AC to feed the AC load. The VSI is controlled with a new PWM based total harmonic distortion (THD) reduction method. MATLAB/SIMULINK platform is used for performance analysis. This work also presents a steady state analysis of a rectifier-inverter topology. Using the method called linearization, the dynamic equations of the proposed system is obtained.; The proposed single switch buck-boost topology provides an output voltage and current of 363V, 45.5A DC from 520V, 35A PV array. The proposed converter is employed to run a 3 Φ induction motor with the rating of 440V, 15A AC. From the simulation results, it is found that the solar powered single switch buck-boost with MPPT is stable, efficient with minimal losses and less THD with better quality output.

Keywords: Solar PV source, Modified P&O algorithm based MPPT, Single switch Buck-boost dc-dc converter, Total Harmonic Distortion, Steady state analysis, Matlab/Simulink

1. INTRODUCTION

Recent years, Renewable energy source powered dc-dc converters have become the most appropriate sources for any kind of power generation because of its abundant availability, less maintenance requirements, pollution free, and lower operational costs. Moreover, solar PV sources have got great attention over other energy sources. To increase the efficiency of the SPV system, MPPT algorithm is much needed. Though there are many MPPT

algorithms in the literature, P&O algorithm is the simplest one which works towards maximum power point using operating point irrespective of the atmospheric conditions, aging, etc., Generally this method compares the SPV current (I_{pv}) and SPV voltage (V_{pv}), introduce delay then controls the values of I_{pv} and V_{pv} , resulting in less system response, fluctuation in finding MPP during steady state [1-3]. To overcome the issue mentioned, this work proposes a modified P&O algorithm that adjusts hysteresis bandwidth & reference step size. It uses hysteresis band and

auto-tuning perturbation step method. Here, the MPPT controllers drive the proposed converter by changing the dc-dc converter duty cycle with variable steps.

According to the authors, Islam et al [4] and Yasmin et al [5], DC/DC/AC converter topologies are mostly preferred in industries and manufacturing companies. In industrial systems, converters with DC-link and battery system, inverters are commonly preferred to provide better power quality, high voltage capability, lesser component stress and lower switching losses [6,7]. It is evident that the stepdown or/ step up converters are used in high power electronic systems for bucking or boosting purposes [8]. Khan et al., [9], Abdikarimuly et al., [10], and Pawar et al., [11] have modelled and simulated various types of buck-boost converters like fly back converter, SEPIC converter and cuk converter. However these converters easily stress the switches, high leakage inductance and less efficiency. Literature [12] also presents KY converters for buck and boost purpose. As the topology uses four power switches and capacitors, in some operational modes, it is suddenly charged. It results a current stress on capacitors, switches and diodes which leads to implementation problems. In this work, the authors propose a novel buck-boost converter topology with a power switch and two capacitors in series. The proposed topology can be operated in continuous conduction mode (CCM) with three different modes. One is ON mode and OFF. OFF mode has two working categories. It will not allow the parallel connected capacitors. The proposed topology uses one power switch, it has the simple control scheme and reduced switching power losses.

As said by the authors Dogga et al., [13] and Aly et al., [14], AC signal conversion from DC signal is done using an inverter with pulse width modulation technique (PWM). PWM signal generation is done with the comparison of a reference signal and a carrier signal. Sinusoidal or square wave signals are considered as reference signal. Saw tooth or a triangular wave signals are taken as carrier signal. PWM signals are generated by triggering the carrier signals by turning ON/OFF the inverter switches. This work uses a sinusoidal PWM technique which further reduces the switching losses [15].

Literature on steady state/ small signal analysis of SPV powered 3 Φ induction motor have been published over the years. It was analysed by the authors [16] and [17]. Root locus technique and frequency dependent method was considered by them. Fallside et al., [18] have analyzed the stability of the proposed system. This method eliminates the effect of harmonics. The stability study of a induction motor based inverter and rectifier system have been analysed by the authors Lipo et al., [19]. This method eliminates stator voltage harmonics. It uses Nyquist stability criterion method. The relationship between voltage and current is considered for the analysis of stability and small signal modelling. Dc-dc converter connected with the inverter and 3 Φ induction motor is considered and their stability is analysed by deriving the d-q voltage-flux-linkage. It has many advantages over

previously discussed methods. Reduced variables are used in the steady state equations. The flux linkages are continuous in nature. It derives a transfer function is derived from the ratio between input and output signals.

The main disadvantages of power electronic loads are harmonics [20,21]. Voltages and currents present in the fundamental frequencies produce harmonics. A lot of literature dealt about the enhancement of power quality using various methods. According to the literature [22-24] there are several techniques which addresses the mitigation of harmonics. THD techniques are classified as passive, active, hybrid passive and active filter etc., Pires et al., [25] found that the passive filter technique is suitable for asymmetrical system having 10kV rating. The authors have used the optimization technique named genetic algorithm (GA) and the Ls and Rs values are taken as objective function. Banaei et al., [26] and Van de Sype et al., [27] have presented a novel passive filter technique for THD reduction. They have followed series and shunt passive filter method where variable impedance controlled by the thyristor is used as shunt filter. The combination of shunt with series type passive filter is called hybrid filter.

Low-voltage networks mostly prefer active harmonic filters due to the limitation posed on power converter rating. This method of harmonic elimination can be used in aircraft power system [28]. Active power filter with the asymmetrical inverter is introduced by the authors An, Le, and Dylan Dah-Chuan Lu [29]. In their findings, at high switching and line frequency is operate at line frequency one leg operated by the inverter legs. High frequency switching can be used to track the compensated current command. Number of researchers have worked to solve time delay problem with the help of neural network (NN) based active filters. p-q and id-iq theory can be controlled instantly with these control technique methods. Chakraborty et al., [30] and Akhil et al., [31] have analyzed p-q and id-iq techniques and also performed a comparative analysis between the techniques. Then they have concluded that better results are achieved by id-iq method. Filters installing methods are so versatile or unique in power electronics topologies. These disadvantages are rejected in switching methods. So this work tries to implement PWM based THD reduction technique.

This work is organized as follows. The first section deals about the view of the previous work done. Second section has block diagram, system description and results discussion of the proposed single switch buck-topology, stability analysis and THD reduction techniques. In third section simulation results and efficiency is discussed. Finally, the findings, disadvantages and the future works of the works are highlighted.

2. BLOCK DIAGRAM OF THE PROPOSED SYSTEM

Fig. 1. presents the pictorial representation of the proposed work. It consists of solar PV power generat-

ing unit, MPPT controller algorithm, single switch buck-boost converter, 3Φ VSI, sinusoidal PWM controller and AC load. SPV system uses a MPPT controller algorithm to track maximum power output. Here modified P&O algorithm based MPPT controller is used.

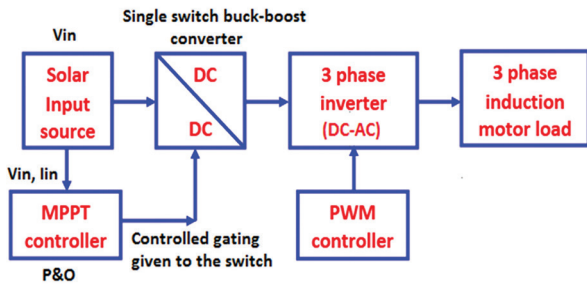


Fig. 1. Block diagram of three phase inverter based Solar PV powered single switch Buck-Boost converter

It utilizes a main inverter circuit to connect dc link to the induction motor. By controlling the switching period of the PWM controller, the inverter using IGBT, reduce harmonics, increase reliability, reduce the complexity, low switching stress power and less cost.

2.1. TOPOLOGY OF THE PROPOSED SYSTEM

The topology of three phase inverter based SPV powered single switch buck-boost converter with reduced THD for industrial applications is presented in Fig.2. It consists of SPV source voltage, single switch buck-boost, battery backup, three phase VSI and 3Φ induction motor.

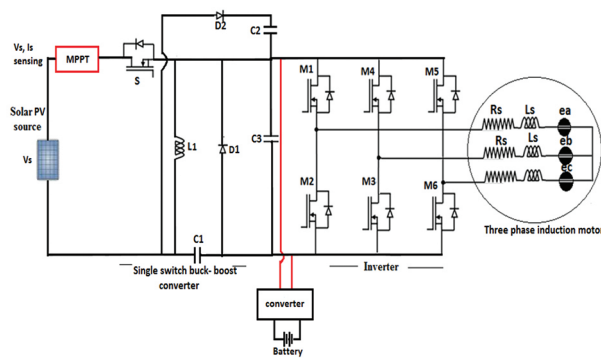


Fig. 2. Topology of the proposed system

2.2. MODELLING OF SOLAR PV SOURCE

SPV system and the single switch buck-boost converter is connected together. Fig.3. presents the equivalent circuit of a SPV cell. The Eq. (1) gives the I-V characteristics of a solar cell,

$$I = I_s - I_d \left[\exp \left(\frac{q * V}{a * k * T} \right) - 1 \right] \quad (1)$$

Where, k is the Boltzman constant (1.3806×10^{-23} J/K), I_s is the Incident sunlight current, q is the electron charge (1.602×10^{-19} C), T is the Temperature of the $p-n$ junction, a is diode ideality constant and I_d is Shockley diode equation. If the availability of SPV power is

lesser/greater than the required dc power, then short-age/ excess energy charges/ discharges the energy storage system respectively. An dc voltage is inverted as ac voltage using three phase VSI. It is used to drive an 3Φ induction motor load torque of 57.3N-m.

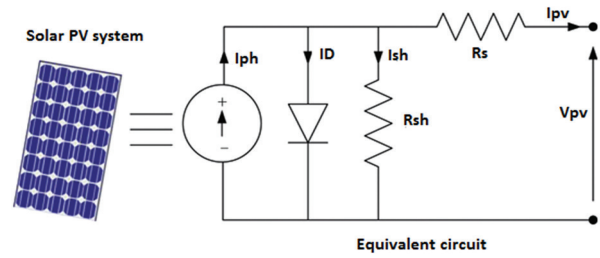


Fig. 3. Solar cell equivalent circuit

SPV system use modified P&O algorithm to track the maximum power obtained from the panel. Gate pulses obtained from the modified algorithms are used as a switching pulses for single switch buck-boost converter. 900 W/m² of insolation, 520V, 35A, 18.2kW is taken for simulation purposes.

The outcome from the simulation SPV voltage, current and power is presented in Fig. 4a, 4b and 4c. From the simulation outcome, it is observed that the obtained total solar power is 18.2 kW.

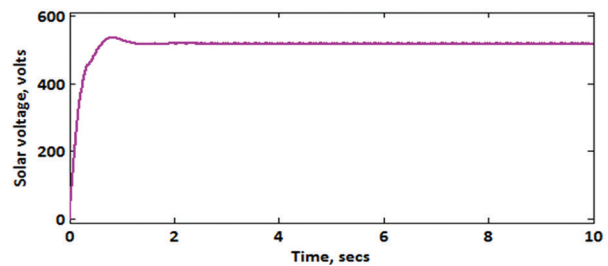


Fig. 4a. Solar voltage

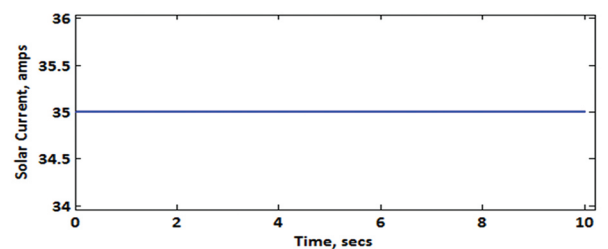


Fig. 4b. Solar current

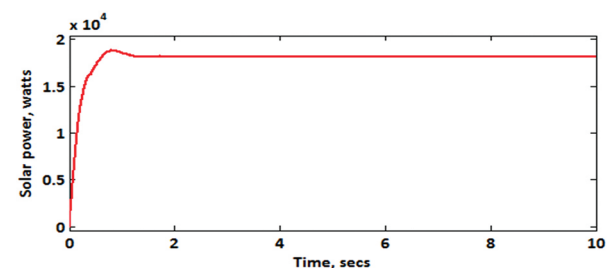


Fig. 4c. Solar power

Modeling of modified P&O algorithm is discussed here. Pictorial representation of the modified P&O is in Fig. 4d. In modified P&O tracking small perturbation is given for the duty cycle modification. This process is repeated till the maximum power is tracked. Till the system finds the steady state and maximum peak point, the algorithm oscillates around.

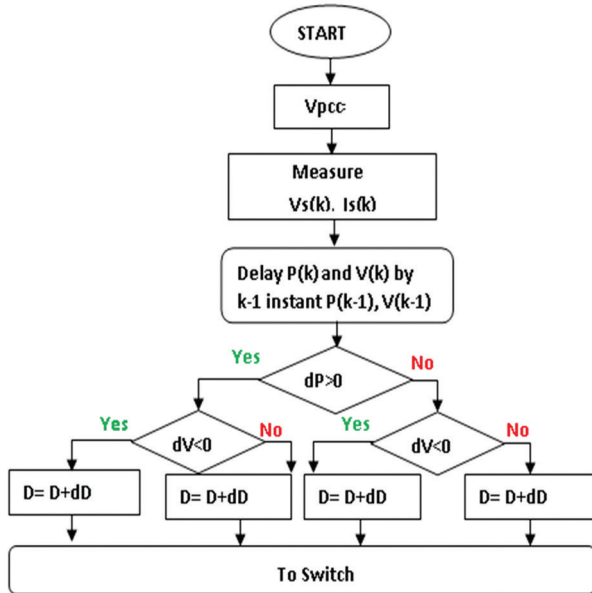


Fig. 4d. Flow chart for modified P & O algorithm

2.3. MODELLING OF 3Φ INDUCTION MACHINE

The electrical and mechanical equations of 3Φ induction machine drive system is expressed as follows,

$$\begin{bmatrix} V_{qs}^e \\ V_{ds}^e \\ V_{qr}^e \\ V_{dr}^e \end{bmatrix} = \begin{bmatrix} r_s + \frac{\rho}{\omega_r} X_{ss} & \frac{\omega_s}{\omega_r} X_{ss} & \frac{\rho}{\omega_r} X_M & \frac{\omega_s}{\omega_r} X_M \\ -\frac{\omega_s}{\omega_r} X_{ss} & r_s + \frac{\rho}{\omega_r} X_{ss} & -\frac{\omega_s}{\omega_r} X_M & \frac{\rho}{\omega_r} X_M \\ \frac{\rho}{\omega_r} X_M & s \frac{\omega_s}{\omega_r} X_M & r_r + \frac{\rho}{\omega_r} X_{rr} & s \frac{\omega_s}{\omega_r} X_{rr} \\ -s \frac{\omega_s}{\omega_r} X_M & \frac{\rho}{\omega_r} X_M & -s \frac{\omega_s}{\omega_r} X_{rr} & r_r + \frac{\rho}{\omega_r} X_{rr} \end{bmatrix} \begin{bmatrix} i_{qs}^e \\ i_{ds}^e \\ i_{qr}^e \\ i_{dr}^e \end{bmatrix} \quad (2)$$

Where, r_r – rotor resistance, r_s – stator resistance, ρ is the operator d/dt , ω_s and ω_r are the base electrical and rotor angular velocity,

$$s = \frac{\omega_s - \omega_r}{\omega_s}, X_{ss} = X_{ls} + X_M \text{ and } X_{rr} = X_{lr} + X_M \quad (3)$$

$$T_e - T_L = J \frac{2}{p} \rho \omega_r$$

$$T_e = \left(\frac{3}{2}\right) \left(\frac{P}{2}\right) \frac{X_M}{\omega_s} (i_{qs}^e * i_{dr}^e - i_{ds}^e * i_{qr}^e) \quad (4)$$

Where, P - number of poles, J - Inertia of the rotor (kg-m²) and T_L, T_e is the load torque and electrical torque of the induction motor.

The configuration model of the proposed single switch buck-boost converter is shown in Fig. (5a). It has one power switch (S), three capacitors (C_1, C_2 & C_3), two inductors (L_1 & L_2) and two diodes (D_1 & D_2).

Various modes of operation of the proposed converter is given in Fig. (5b). It has three modes of operation.

When the switch S is in ON position, it is Mode-1. OFF position of the switch has two modes named Mode-2 and Mode-3. With the capacitors named C_2 and C_3 in the topology, dc load is connected. This makes the dc output voltage as two times $D/(1-D)$ that of the input voltage.

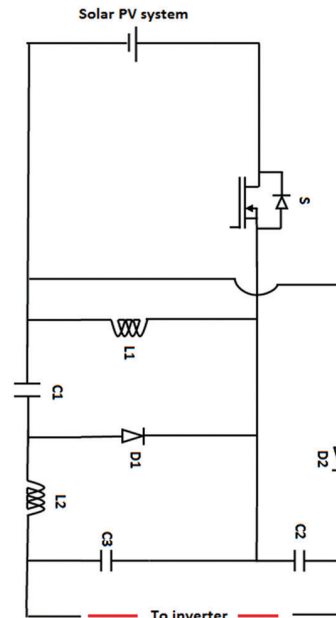


Fig. 5a. Topology of the single switch buck-boost converter

a. Mode 1: Switch S - ON condition

Fig. (6a). shows the Mode-1 operation (S is ON). Switch S is conducting which turns off the diodes D_1 and D_2 . So D_1 and D_2 are in reverse biased. Then inductor L_1 is magnetized through the solar PV source. Capacitors C_1 and C_3 are used to magnetize/charge the inductor L_2 . Capacitors C_2 and C_3 feeds the load or energy deposited in the capacitors C_2 and C_3 are demagnetized through the load. In Fig. (6a), Applying KVL to the loops following equations are obtained.

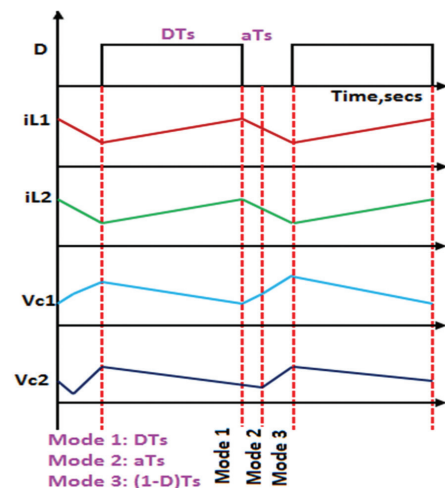


Fig. 5b. Modes of operation

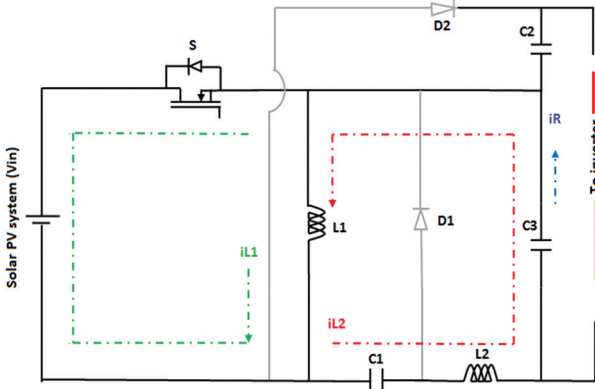


Fig. 6a. Mode-1 S- ON

$$\frac{di_{L1}}{dt} = \frac{1}{L_1} V_{in} \quad (5)$$

$$\frac{di_{L2}}{dt} = \frac{1}{L_2} (V_{in} + V_{C1} - V_{C3}) \quad (6)$$

$$V_{Load} = V_{C2} + V_{C3} \quad (7)$$

By applying KCL to the circuit, the current flows through the capacitors are obtained

$$I_{C1} = -I_{L2} \quad (8)$$

$$I_{C2} = -I_R \quad (9)$$

$$I_R = I_{L1} - \frac{C_1 + C_2}{C_1} I_{C1} \quad (10)$$

$$\begin{bmatrix} \frac{dV_{C1}}{dt} \\ \frac{dV_{C2}}{dt} \\ \frac{dV_{C3}}{dt} \\ \frac{di_{L1}}{dt} \\ \frac{di_{L2}}{dt} \end{bmatrix} = \begin{bmatrix} 0 & 0 & 0 & 0 & -\frac{1}{C_1} \\ 0 & 0 & 0 & -\frac{1}{C_2} & 0 \\ \frac{C_1 + C_2}{C_1} & 0 & 0 & 0 & 0 \\ 0 & 0 & 0 & 0 & 0 \\ \frac{1}{L_2} & 0 & -\frac{1}{L_2} & 0 & 0 \end{bmatrix} * \begin{bmatrix} V_{C1} \\ V_{C2} \\ V_{C3} \\ i_{L1} \\ i_{L2} \end{bmatrix} + \begin{bmatrix} 0 \\ 0 \\ 1 \\ 1 \\ 1 \end{bmatrix} * \begin{bmatrix} 0 \\ 0 \\ 0 \\ 1 \\ 1 \end{bmatrix} \quad (11)$$

$$[0 \ 0 \ 0 \ V_1 \ V_2]$$

Where $A_1 = \begin{bmatrix} 0 & 0 & 0 & 0 & -\frac{1}{C_1} \\ 0 & 0 & 0 & -\frac{1}{C_2} & 0 \\ \frac{C_1 + C_2}{C_1} & 0 & 0 & 0 & 0 \\ 0 & 0 & 0 & 0 & 0 \\ \frac{1}{L_2} & 0 & -\frac{1}{L_2} & 0 & 0 \end{bmatrix}$ and $B_1 = \begin{bmatrix} 0 \\ 0 \\ 1 \\ 1 \\ 1 \end{bmatrix}$

b. Mode 2: Switch S - OFF condition.

Fig. 6b shows the Mode-2 operation. Switch S is in non-conducting condition which turns on the diode D1 and diode D2 is still in off position. It makes the diode D1 in biased forward mode and D2 in reverse biased condition. In this mode, capacitors C1 is demagnetizing the inductors L1 and L2. It also charges the capacitor C3.

Energy that are stored already in the capacitor C2 is discharged through the load. This mode continues till the charge in capacitor C1 is equal to capacitor C2. This avoids the current spikes through capacitors and diodes. In Fig. 6b, Applying KVL to the loops following equations are obtained.

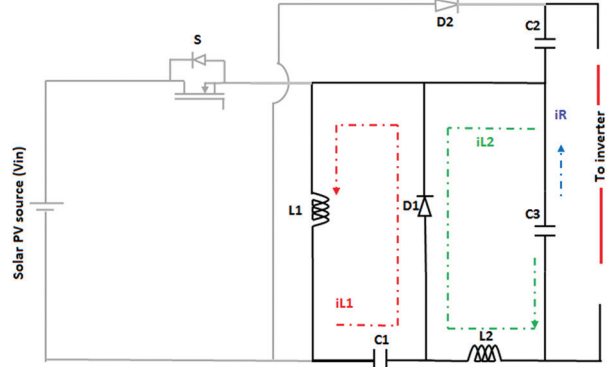


Fig. 6b. Mode-2 S-OFF

$$\frac{di_{L1}}{dt} = -\frac{1}{L_1} V_{C1} \quad (12)$$

$$\frac{di_{L2}}{dt} = -\frac{1}{L_2} V_{C3} \quad (13)$$

$$V_{Load} = V_{C2} + V_{C3} \quad (14)$$

By applying KCL to the circuit, the current flows through the capacitors are obtained

$$I_{C1} = I_{L1} \quad (15)$$

$$I_{C2} = -I_R \quad (16)$$

$$I_R = I_{L1} - \frac{C_1 + C_2}{C_1} I_{C2} \quad (17)$$

$$\begin{bmatrix} \frac{dV_{C1}}{dt} \\ \frac{dV_{C2}}{dt} \\ \frac{dV_{C3}}{dt} \\ \frac{di_{L1}}{dt} \\ \frac{di_{L2}}{dt} \end{bmatrix} = \begin{bmatrix} 0 & 0 & 0 & \frac{1}{C_1} & 0 \\ 0 & 0 & 0 & -\frac{1}{C_2} & 0 \\ \frac{C_1 + C_2}{C_1} & 0 & -1 & 0 & 0 \\ \frac{1}{L_1} & 0 & 0 & 0 & 0 \\ \frac{1}{L_2} & 0 & -\frac{1}{L_2} & 0 & 0 \end{bmatrix} * \begin{bmatrix} V_{C1} \\ V_{C2} \\ V_{C3} \\ i_{L1} \\ i_{L2} \end{bmatrix} + \begin{bmatrix} 0 \\ 0 \\ 1 \\ 1 \\ 1 \end{bmatrix} * \begin{bmatrix} 0 \\ 0 \\ 0 \\ 1 \\ 1 \end{bmatrix} \quad (18)$$

$$[0 \ 0 \ 0 \ V_1 \ V_2]$$

Where $A_2 = \begin{bmatrix} 0 & 0 & 0 & \frac{1}{C_1} & 0 \\ 0 & 0 & 0 & -\frac{1}{C_2} & 0 \\ \frac{C_1 + C_2}{C_1} & 0 & -1 & 0 & 0 \\ \frac{1}{L_1} & 0 & 0 & 0 & 0 \\ \frac{1}{L_2} & 0 & -\frac{1}{L_2} & 0 & 0 \end{bmatrix}$ and $B_2 = \begin{bmatrix} 0 \\ 0 \\ 1 \\ 1 \\ 1 \end{bmatrix}$

c. Mode 3: Switch S is still in OFF condition.

Fig. (6c). shows the Mode-position. Switch S is in non-conducting mode and the charge remaining in capacitor C₁ is equal to C₂. It turns on the diodes D₁ and D₂. So D₁ & D₂ are in forward biased. In this mode, inductor L₁ is demagnetized through C₁ and C₂. Inductor L₂ charges the capacitor C₃. Energy that are stored already in the capacitor C₂ is discharged via dc load.

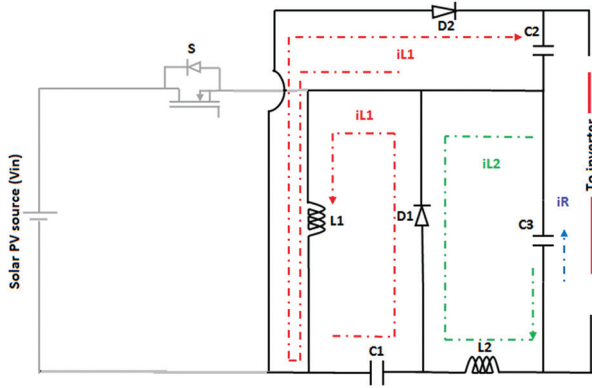


Fig. 6c. Mode- 2 S-OFF

$$\frac{di_{L1}}{dt} = -\frac{1}{L_1} V_{C1} \quad (19)$$

$$\frac{di_{L2}}{dt} = -\frac{1}{L_2} V_{C3} \quad (20)$$

$$\begin{bmatrix} \frac{dV_{C1}}{dt} \\ \frac{dV_{C2}}{dt} \\ \frac{dV_{C3}}{dt} \\ \frac{di_{L1}}{dt} \\ \frac{di_{L2}}{dt} \end{bmatrix} = \begin{bmatrix} 0 & 0 & 0 & \frac{1}{C_1} & 0 \\ 0 & 0 & 0 & -\frac{1}{C_2} & 0 \\ C_1 + C_2 & -1 & 0 & 0 & 0 \\ \frac{1}{L_1} & 0 & 0 & 0 & 0 \\ \frac{1}{L_2} & 0 & -\frac{1}{L_2} & 0 & 0 \end{bmatrix} \begin{bmatrix} V_{C1} \\ V_{C2} \\ V_{C3} \\ i_{L1} \\ i_{L2} \end{bmatrix} + \begin{bmatrix} 0 \\ 0 \\ 1 \\ \frac{1}{L_1} \\ \frac{1}{L_3} \end{bmatrix} \begin{bmatrix} 0 \\ 0 \\ 0 \\ 0 \\ 0 \end{bmatrix} \quad (21)$$

Where $A_3 = \begin{bmatrix} 0 & 0 & 0 & \frac{1}{C_1} & 0 \\ 0 & 0 & 0 & -\frac{1}{C_2} & 0 \\ C_1 + C_2 & -1 & 0 & 0 & 0 \\ \frac{1}{L_1} & 0 & 0 & 0 & 0 \\ \frac{1}{L_2} & 0 & -\frac{1}{L_2} & 0 & 0 \end{bmatrix}$ and $B_3 = \begin{bmatrix} 0 \\ 0 \\ 1 \\ \frac{1}{L_1} \\ \frac{1}{L_3} \end{bmatrix}$

The proposed single switch buck-boost converter is assumed to be CCM mode. Let us assume the switch S1 is in the ON position individually for the time period d1TS & d2TS. Switch S1 is in OFF position for the time period (1- d1) TS & (1- d2) TS. In this case d1 and d2 are taken as the duty cycle and TS is considered as the switching duration. Here the capacitor voltages (VC1

and VC2) are equal and the average inductor current (IL2) is same as the output current. The inductor time constant is stated as,

$$t_L = \frac{1}{2} (1 - D)^2 \quad (22)$$

By applying volt-sec balance equation on inductor L₁

$$DV_{in} - \alpha V_{C1} - ((1 - D - \alpha)(V_{C1})) = 0 \quad (23)$$

By solving this equation,

$$V_{C1} = V_{C2} = V_{in} \frac{D}{1 - D} \quad (24)$$

Volt-sec balance equation is applied on inductor L₂,

$$D(V_{in} + V_{C1} - V_{C3}) - \alpha V_{C3} - ((1 - D - \alpha)(V_{C3})) = 0 \quad (25)$$

By solving this equation,

$$V_{C3} = V_{in} \frac{D}{1 - D} \quad (26)$$

By applying ampere-sec balance equation on capacitor C₁,

$$-(D + \alpha)(I_R) + \left((1 - D - \alpha) \left(\frac{C_1}{C_1 + C_2} (I_{L1} - I_R) \right) \right) = 0 \quad (27)$$

Ampere-sec balance equation is applied on capacitor C₂,

$$-(D + \alpha)(I_R) + \left((1 - D - \alpha) \left(\frac{C_1}{C_1 + C_2} (I_{L1} - I_R) \right) \right) = 0 \quad (28)$$

By solving these equations,

$$I_{L2} = I_R \quad (29)$$

The proposed system is operated at CCM operation. So the average voltage of the proposed system is calculated as follows,

$$\frac{V_{C2}}{V_{in}} = \frac{2D}{1 - D} \quad (30)$$

During transient period, the inductor voltage and current, capacitor voltage and current and dc voltage and current may vary due to time. For any dc-dc converter having commutating capacitance, inductance and with no phase delay is,

$$V_{dc} = V_d + X_{Ldc} \rho I_d \quad (31)$$

$$\rho V_{dc} = \omega_b X_{Cdc} (I_d - I_{dc}) \quad (32)$$

$$V_d = \left(\frac{3\sqrt{3}}{\pi} V_q^G \right) - \left(\frac{3 X_{Lc}}{\pi \omega_b} \omega_{e0} I_d \right) - \frac{2}{\omega_b} X_{Lc} \rho I_d \quad (33)$$

Substituting the equation (33) in (31),

$$V_{dc} = \left(\frac{3\sqrt{3}}{\pi} V_q^G \right) - \left(\frac{3 X_{Lc}}{\pi \omega_b} \omega_g I_d \right) - \frac{1}{\omega_b} (X_{Lc} + 2X_{Lc}) \rho I_d \quad (34)$$

Where, V_q^G - q component of the dc voltage and ω_g - system frequency, d- duty cycle of modulation.

Neglecting the harmonics in the VSI source with sin-triangle pulse width modulation, voltages in the rotating reference frame become,

$$V_{qs}^e = \frac{d}{2} V_{dc} \quad (35)$$

$$V_{ds}^e = 0 \quad (36)$$

The power balance equation is,

$$V_{dc} * I_{dc} = \left(\frac{3}{2}\right) V_{qs}^e I_{qs}^e \quad (37)$$

$$I_{dc} = \left(\frac{3d}{4}\right) I_{qs}^e \quad (38)$$

$$\rho V_{dc} = \omega_b X_{Cdc} \left(I_d - \left(\frac{3d}{4}\right) I_{qs}^e \right) \quad (39)$$

The above equations are the dynamic equations of DC system.

d. Design equations of the proposed converter

The parameter value of the components inductor and capacitor is calculated as follows,

$$\Delta I_{L1} = \frac{V_{in} D}{L_1 f} \quad (40)$$

$$\Delta I_{L2} = \frac{V_{C3} D}{L_2 f} \quad (41)$$

$$\Delta V_{C1} = \frac{I_{in} (1 - D)}{C_1 f} \quad (42)$$

$$\Delta V_{C2} = \frac{I_R (1 - D)}{C_2 f} \quad (43)$$

$$\Delta V_{C3} = \frac{I_R (1 - D)}{C_3 f} \quad (44)$$

From the above equations (40) to (44), the simulation parameters are calculated and the circuit is simulated. Let the duty cycle $D=0.74$, input voltage $V_{in} = 520V$, input current $I_{in}=35A$ and frequency $f= 20kHz$

Table.1. Simulation parameters

Components	Values
L1	400 μH
L2	84.16 μH
C1	0.01 μF
C2	0.01 μF
C3	0.01 μF
Input	520V, 35A
Switching frequency	20kHz

Backup power can be compensated load demand when needed.

2.5. REDUCTION OF THD IN 3PHASE INVERTER TOPOLOGY

Fig. 7. Presents the proper layout of three phase VSI. It has six controlled semiconductor switches. By controlling the switching pattern, the output ac voltage and line currents can be obtained as pure sinusoidal. Instead of using installing active/ passive filters. Some of the harmonics are eliminated using switching pattern techniques. PWM is a different switching technique which gives versatile results by varying modulation ratio and index and switching frequency. Here increasing the switching frequency can reduce the current harmonics which further increases the switching losses. THD is very much useful in finding the harmonics order presented in the voltage or current waveforms. It helps in observing the quality of non-sinusoidal wave. THD is the division between all harmonic components RMS value and the fundamental component RMS.

$$THD = \frac{\sqrt{\sum_{n=2}^{\infty} V_{n,rms}^2}}{V_{fund,rms}} \quad (45)$$

Where, $V_{n,rms}$ is the nth harmonic RMS voltage and $V_{fund,rms}$ is the RMS voltage of the fundamental frequency.

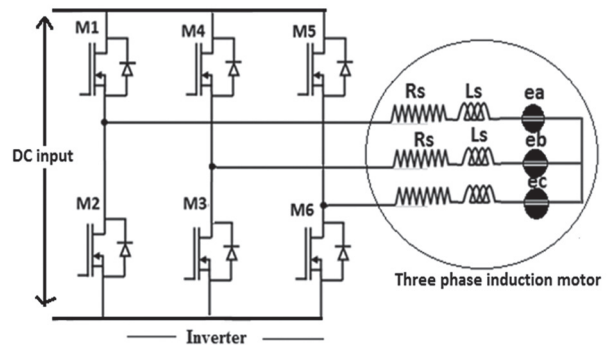


Fig. 7. Three phase inverter with 3 Φ induction motor

In this work, the steady state analysis of the proposed system have been performed. Linearization of systems about an operating point with nonlinear differential equations are taken. The small signal model of linearization of mechanical equation of induction motor is given by,

$$J \Delta \omega_b \rho = \left(\frac{3}{2\omega_b}\right) \left(\frac{P}{2}\right)^2 \left(\begin{matrix} X_M I_{qs0}^e \Delta I_{dr}^e + X_M \Delta I_{qs}^e I_{dr0}^e \\ -X_M I_{ds0}^e \Delta I_{qr}^e - X_M \Delta I_{ds}^e I_{qr0}^e \end{matrix} \right) - \frac{P}{2} \Delta T_L \quad (46)$$

Here 0 denotes the steady state quantities at an operating point. The fundamental form of the linear differential equation is

$$\rho \Delta X = A \Delta X + B \Delta U \quad (47)$$

Where, $A=E^{-1} F$, $B=E^{-1} B' F$, ΔX and ΔU are state and control variables. A is the state matrix of the proposed system.

$$E = \frac{1}{\omega_b} \begin{bmatrix} X_{SS} & 0 & X_M & 0 & 0 & 0 & 0 \\ 0 & X_{SS} & 0 & X_M & 0 & 0 & 0 \\ X_M & 0 & X_{rr} & 0 & 0 & 0 & 0 \\ 0 & 0 & 0 & X_{rr} & 0 & 0 & 0 \\ 0 & 0 & 0 & 0 & J\omega_b & 0 & 0 \\ 0 & 0 & 0 & 0 & 0 & 1 & 0 \\ 0 & 0 & 0 & 0 & 0 & 0 & \omega_b \end{bmatrix} \quad (48)$$

$$B' = \begin{bmatrix} 0 & 0 & 0 & 0 & 0 & 0 \\ 0 & 0 & 0 & 0 & 0 & 0 \\ 1 & 0 & 0 & 0 & 0 & 0 \\ 0 & 1 & 0 & 0 & 0 & 0 \\ 0 & 0 & -\frac{P}{2} & 0 & 0 & 0 \\ 0 & 0 & 0 & 0 & 0 & 0 \\ 0 & 0 & 0 & \frac{3\sqrt{3}}{\pi(X_{Ldc} + 2X_{Lc})} \omega_b & 0 & -\frac{3X_{Lc}I_{d0}}{\pi(X_{Ldc} + 2X_{Lc})} \end{bmatrix} \quad (49)$$

Linear combination of state and control variables form output vector of the system,

$$\Delta Y = C\Delta X + D\Delta U \quad (50)$$

In induction motor electromagnetic torque T_e and rotor velocity ω_r are considered as output.

$$\Delta T_\theta = C_1\Delta X + D_1\Delta U \quad (51)$$

Where,

$$C_1 = \frac{3P}{4\omega_b} X_M [I_{dr0}^e \quad -I_{qr0}^e \quad -I_{ds0}^e \quad I_{qs0}^e \quad 0 \quad 0 \quad 0]$$

$$D_1 = [0 \quad 0 \quad 0 \quad 0 \quad 0 \quad 0 \quad 0]$$

$$\Delta\omega_r = C_2\Delta X + D_2\Delta U \quad (52)$$

Where,

$$C_2 = [0 \quad 0 \quad 0 \quad 0 \quad 1 \quad 0 \quad 0]$$

$$D_2 = [0 \quad 0 \quad 0 \quad 0 \quad 0 \quad 0 \quad 0]$$

With the state and output equations, the transfer function of the system is written as,

$$\frac{\Delta Y}{\Delta U} = C(SI - A)^{-1}B + D \quad (53)$$

The steady state currents are given as,

$$\begin{bmatrix} i_{qs}^e \\ i_{ds}^e \\ i_{qr}^e \\ i_{dr}^e \end{bmatrix} = \begin{bmatrix} r_s & \frac{\omega_s}{\omega_r} X_{SS} & 0 & \frac{\omega_s}{\omega_r} X_M \\ -\frac{\omega_s}{\omega_r} X_{SS} & r_s & -\frac{\omega_s}{\omega_r} X_M & 0 \\ 0 & s\frac{\omega_s}{\omega_r} X_M & r_r & s\frac{\omega_s}{\omega_r} X_{rr} \\ -s\frac{\omega_s}{\omega_r} X_M & 0 & -s\frac{\omega_s}{\omega_r} X_{rr} & r_r \end{bmatrix} \begin{bmatrix} V_{qs}^e \\ V_{ds}^e \\ V_{qr}^e \\ V_{dr}^e \end{bmatrix} \quad (54)$$

Table 2 show the induction motor specifications.

Table 2. Simulation parameters of induction motor

Parameters	Values
Power	18kW
Voltage	440V
Speed	1820rpm
Stator and rotor resistance	0.214Ω and 0.22 Ω
Xls and Xlr	9e-3H and 9e-3H
Mutual inductance	0.0114H
Inertia(J)	0.102Kg/m ²

3. DISCUSSION ON SIMULATION RESULTS

To analyze the proposed single switch buck-boost topology based 3Φ induction motor, a detailed MATLAB/SIMULINK is carried out in R2013a version. The dc link voltage is set at 360V and the dc link current at 45A. Fig. 8a and 8b shows the current and voltage across the dc load. It is noted that the voltage across topology is measured as 363V and the current through the topology is measured as 45.5A.

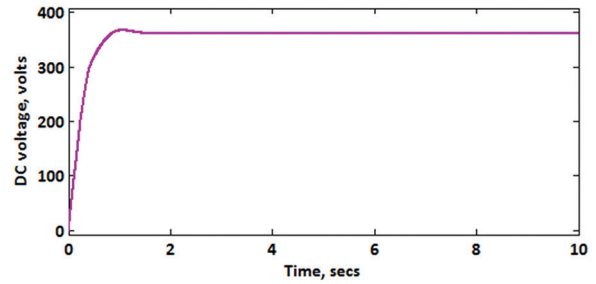


Fig. 8a. Voltage across DC load

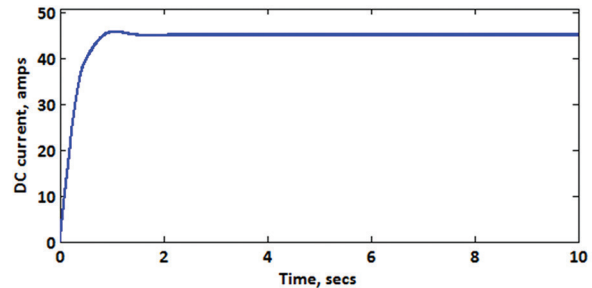


Fig. 8b. Current through DC load

Fig. 9a and 9b presents the ac output voltage and current of three phase inverter respectively. From the graph, it is noted that 440V of output voltage and 15A of output current is observed.

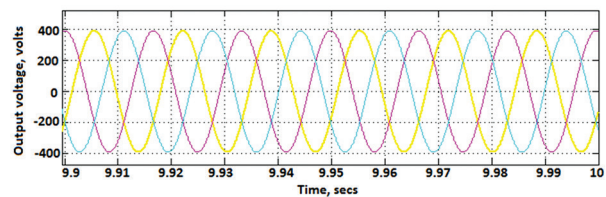


Fig. 9a. AC output voltage

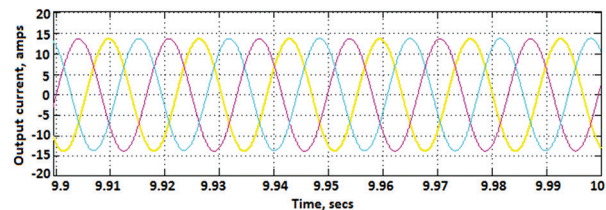


Fig. 9b. AC output current

Fig. 10 shows the results of gate pulse generation process in three phase inverter circuit. Here, two sine waves

are joined to generate the reference signal. Switching loss of the inverter can be eliminated by using three times frequency of the sine wave compared to other. It cancels the harmonics by utilizing the dc supply more. It also shows the switching pulses of inverter switches.

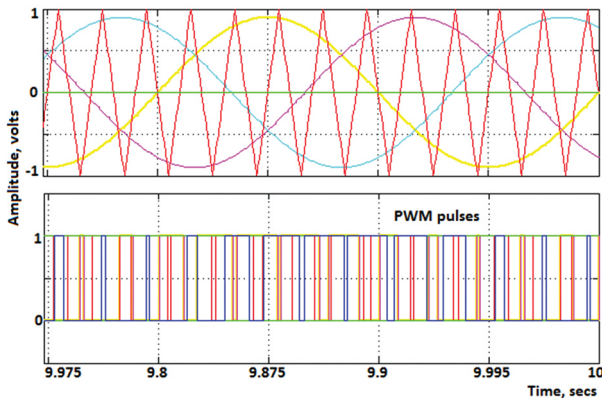


Fig.10. Gate pulse generation of inverter switches

Fig.11 and 12 shows the motor speed and T_e (electromagnetic torque).

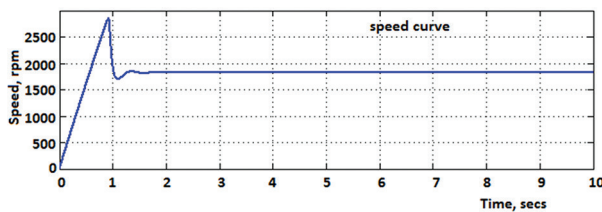


Fig. 11. Motor speed

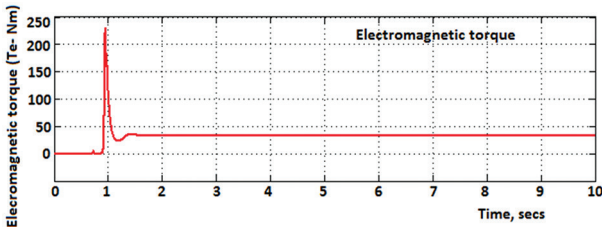


Fig. 12. Electromagnetic torque (T_e)

The obtained transfer function mentioned in equation (53) is done using MATLAB/SIMULINK, R2013a version with the same simulation values for investigating its stability. By using LQG controller, it performs many attempts for the designed closed loop model. The time domain and frequency domain responses of the system are observed. The step and impulse response is shown in Fig. 13 a and 13 b. From the step response figure, zero overshoot, no peak and no transients is seen in the closed loop. Impulse response figure shows 1.01 peak response with zero overshoot. The settling time is 0.3 sec. Fig. 14 a and 14 b shows the frequency response of the system.

The main condition for the stable system in root locus is that the placement of the poles and zeros should be

on the left hand side. It can be able to provide response characteristics of the system. From the obtained result of the proposed system with LQG synthesis controller, it is shown that the system is stable with the gain and phase margins of -0.0202 dB, 0.0374 rad/sec and 0.737 deg, 47.7 rad/sec respectively.

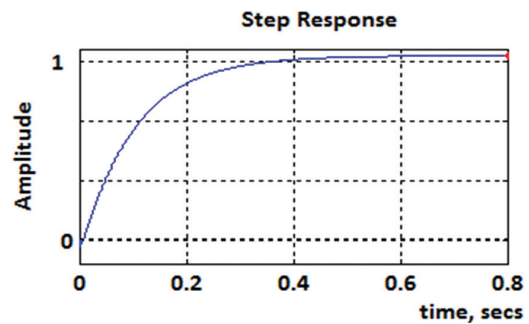


Fig. 13a. Step response

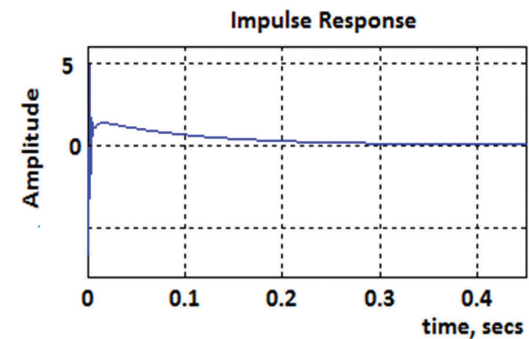


Fig. 13 b. Impulse response

Then performance analysis is carried out depending on the value of THD %. Deviation in the THD is read by changing the frequency and modulation index of the carrier signal. The obtained THD values of output current and voltage is shown in Fig.15 a and 15 b in which we got the THD values of 5.43% and 7.14% respectively. Efficiency of the proposed converter is the total output voltage divided by the input voltage. It is obtained as $[(363 \times 45.5) / (520 \times 35)] \times 100 = 90.5\%$.

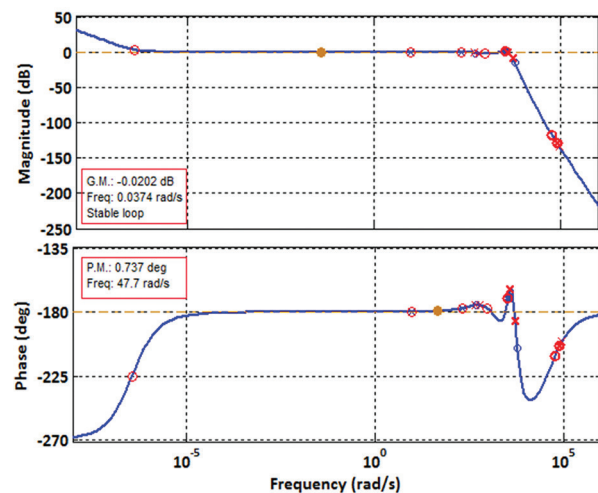


Fig. 14 a. Frequency response- Bode plot

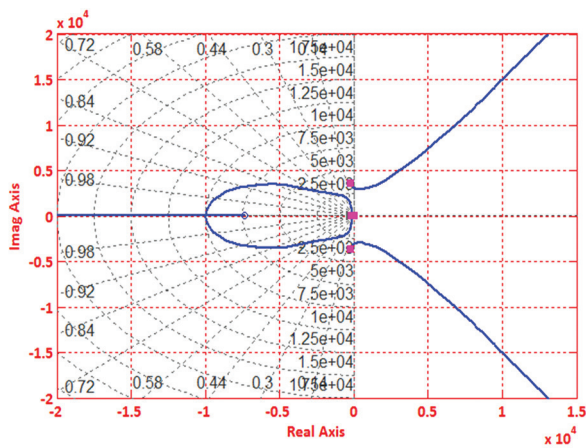


Fig. 14 b. Frequency response- Pole-Zero plot

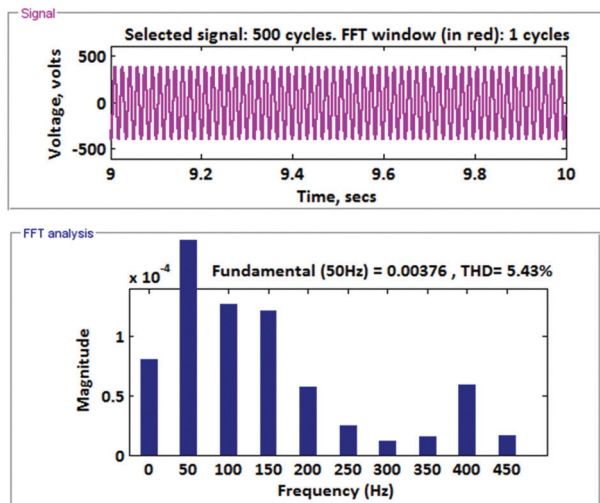


Fig. 15 a. THD of AC Output voltage

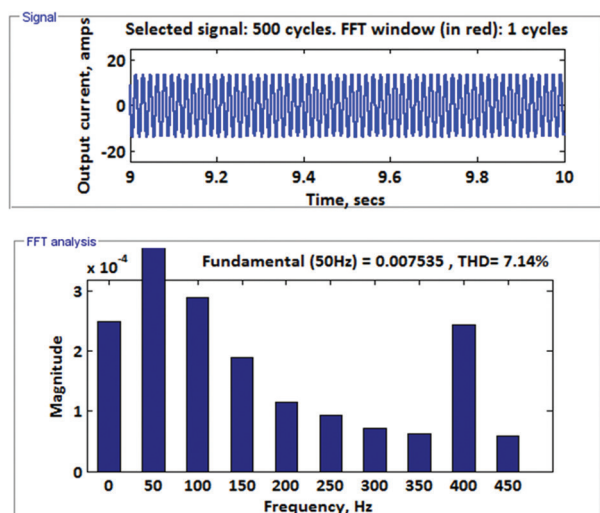


Fig. 15 b. THD of AC output current

4. CONCLUSION

Solar PV powered single switch buck-boost converter is simulated with reduced cost, minimal voltage and current stress across the capacitors and diodes, less

switching power losses and increased efficiency. In this work solar PV source with modified P & O algorithm based MPPT, single switch buck-boost dc-dc converter, battery backup to store excess energy, three phase inverter with sinusoidal PWM to find optimal switching angles for harmonic control and 3 Φ induction motor load is used. Reduction of THD is applied to the line to line voltage and current of the inverter and observed the voltage and current THD of 5.43% and 7.14% respectively. Performance analysis of the topology proposed is done using MATLAB/SIMULINK 2013a platform. The proposed single switch buck-boost converter has produced an output voltage and current of 363V, 45.5A DC from 520V, 35A PV array. The designed converter is then connected with a three phase VSI with 440V, 15A AC. The obtained efficiency is 90.5%. Here small signal steady state analysis is performed for the proposed system. In the extension of this work several new strategies in the MPPT algorithms like Ant colony, firefly etc., can be preferred. Recent control algorithms for VSI can be used. Fault analysis of 3 Φ induction motor can be performed.

5. REFERENCES:

- [1] M. R. Banaei, H. Ardi, A. Farakhor, "Analysis and implementation of a new single-switch buck-boost DC/DC converter", IET Power Electronics, Vol. 7, No. 7, 2014, pp. 1906-1914.
- [2] S.-Y. Tseng, J.-H. Fan, "Buck-Boost/Fly back Hybrid Converter for Solar Power System Applications", Electronics, Vol. 10, No.4, 2021, p. 414.
- [3] J. M. Alonso, J. Vina, D. G. Vaquero, G. Martinez, R. Osorio, "Analysis and design of the integrated double buck-boost converter as a high-power-factor driver for power-LED lamps", IEEE Transactions on Industrial Electronics, Vol. 59, No. 4, 2011, pp. 1689-1697.
- [4] Md T. Islam, S. I. Ayon, "Performance Analysis of Three-Phase Inverter for Minimizing Total Harmonic Distortion Using Space Vector Pulse Width Modulation Technique", Proceedings of the 23rd International Conference on Computer and Information Technology, Dhaka, Bangladesh, 19-21 December 2020, pp. 1-4.
- [5] F. Yalcin, U. Arifoglu, I. Yazici, K. Erin, "Robust single-phase inverter based on the buck-boost converter through an efficient hybrid control", IET Power Electronics, Vol. 13, No. 1, 2020, pp. 50-59.
- [6] M. Schubert, R. W. De Doncker. "Instantaneous phase voltage sensing in PWM voltage-source

- inverters", *IEEE Transactions on Power Electronics*, Vol. 33, No. 8, 2017, pp. 6926-6935.
- [7] T. T. Atly, "Notice of Removal: Active buck-boost inverter for inverter air conditioner applications", *Proceedings of the International Conference on Electrical, Electronics, Signals, Communication and Optimization*, Visakhapatnam, India, 24-25 January 2015, pp. 1-5.
- [8] M. E. Ibrahim, A. S. Mansour, A. M. Abd-Elhady, "A novel single-stage single-phase buck-boost inverter", *Electrical Engineering*, Vol. 99, No. 1, 2017, pp. 345-356.
- [9] M. M. S. Khan, Md S. Arifin, Md R. T. Hossain, Md A. Kabir, A. H. Abedin, M. A. Choudhury, "Input switched single phase buck and buck-boost AC-DC converter with improved power quality", *Proceedings of the 7th International Conference on Electrical and Computer Engineering*, Dhaka, Bangladesh, 20-22 December 2012, pp. 189-192.
- [10] R. Abdikarimuly, A. Ruderman, B. Reznikov, "Calculation of current total harmonic distortion for a three-phase two-level inverter with LCL-filter", *Proceedings of the 19th International Conference on Electrical Drives and Power Electronics*, Dubrovnik, Croatia, 4-6 October 2017, pp. 100-105.
- [11] P. S. Pawar, J. S. Bagi, G. R. Shinde, "A Review on Harmonic Reduction Techniques in Three-Phase Power Generation in PV Solar Plants", *International Journal of Electrical and Electronics Engineering*, Vol. 9, No. 1, 2019, pp. 1-6.
- [12] P. J. B. Rao, B. Srikanth, "Harmonic reduction in grid connected solar PV system by using SVPWM technique", *International Journal of Applied Engineering Research*, Vol. 11, No. 6, 2016, pp. 3853-3858.
- [13] R. Dogga, M. K. Pathak, "Recent trends in solar PV inverter topologies", *Solar Energy*, Vol. 183, 2019, pp. 57-73.
- [14] M. Aly, H. A. Ramadan, "Design and implementation of adaptive SVPWM algorithm for multilevel inverters in renewable energy applications", *Solar Energy*, Vol. 183, 2019, pp. 745-754.
- [15] R. Barzegarkhoo, E. Zamiri, N. Vosoughi, H. M. Kojabadi, L. Chang, "Cascaded multilevel inverter using series connection of novel capacitor-based units with minimum switch count", *IET Power Electronics*, Vol. 9, No. 10, 2016, pp. 2060-2075.
- [16] P. C. Krause, T. A. Lipo, "Analysis and simplified representations of a rectifier-inverter induction motor drive", *IEEE Transactions on Power Apparatus and Systems*, Vol. PAS-88, No. 5, 1969, pp. 588-596.
- [17] R. H. Nelson, T. A. Lipo, P. Krause, "Stability analysis of a symmetrical induction machine", *IEEE Trans. Power Apparatus and Systems*, Vol. PAS-88, No. 11, 1969, pp. 1710-1717.
- [18] F. Fallside, A. T. Wortley, "Steady-state oscillations and stabilization of variable frequency inverter fed induction motor drives", *IEEE Proceedings*, Vol. 116, No. 6, 1969, pp. 991-999.
- [19] T. A. Lipo, P. Krause, "Stability analysis of a rectifier-inverter induction motor drives", *IEEE Transactions on Power Apparatus and Systems*, Vol. PAS-88, No. 1, 1969, pp. 55-66.
- [20] V. F. Pires, A. Cordeiro, D. Foito, J. F. Silva, "Three-phase multilevel inverter for grid-connected distributed photovoltaic systems based in three three-phase two-level inverters", *Solar Energy*, Vol. 174, 2018, pp. 1026-1034.
- [21] M. Jayabalan, B. Jeevarathinam, T. Sandirasegarane, "Reduced switch count pulse width modulated multilevel inverter", *IET Power Electronics*, Vol. 10, No. 1, 2017, pp. 10-17.
- [22] V. F. Pires, D. Foito, A. Cordeiro, J. F. Silva, "A single-switch DC/DC buck-boost converter with extended output voltage", *Proceedings of the 7th International Conference on Renewable Energy Research and Applications*, Paris, France, 14-17 October 2018, pp. 791-796.
- [23] M. R. Banaei, H. Ardi, A. Farakhor, "Analysis and implementation of a new single-switch buck-boost DC/DC converter", *IET Power Electronics*, Vol. 7, No. 7, 2014, pp. 1906-1914.
- [24] M. Delshad, H. Farzanehfard, "A new single switch Buck-Boost type dc-dc converter", *Proceedings of the IEEE Symposium on Industrial Electronics & Applications*, Vol. 2, Kuala Lumpur, Malaysia, 4-6 October 2009, pp. 823-826.
- [25] V. F. Pires, D. Foito, A. Cordeiro, J. F. Silva, "A single-switch DC/DC buck-boost converter with extend-

- ed output voltage”, Proceedings of the 7th International Conference on Renewable Energy Research and Applications, Paris, France, 14-17 October 2018, pp. 791-796.
- [26] M. R. Banaei, H. Ardi, F. Bonab, “A novel structure for single-switch non- isolated transformer less buck–boost DC–DC converter”, IEEE Transactions on Industrial Electronics, Vol. 64, No. 1, 2016, pp. 198-205.
- [27] D. M. Van de Sype, K. De Gussemé, W. R. Ryckaert, A. P. Van de Bossche, J. A. Melkebeek, “A single switch buck-boost converter with a high conversion ratio”, Proceedings of the European Conference on Power Electronics and Applications, Dresden, Germany, 11-14 September 2005, p. 10.
- [28] E. Jamshidpour, S. Jovanovic, P. Poure, “Equivalent Two Switches and Single Switch Buck/Buck-Boost Circuits for Solar Energy Harvesting Systems”, Energies, Vol. 13, No. 3, 2020, p. 583.
- [29] L. An, D. D.-C. Lu, “Design of a single-switch DC/DC converter for a PV-battery-powered pump system with PFM+ PWM control”, IEEE Transactions on Industrial Electronics, Vol. 62, No. 2, 2014, pp. 910-921.
- [30] S. Chakraborty, S. I. Annie, M. A. Razzak, “Design of single-stage buck and boost converters for photovoltaic inverter applications”, Proceedings of the International Conference on Informatics, Electronics & Vision, Dhaka, Bangladesh, 23-24 May 2014, pp. 1-6.
- [31] M. M. Akhil, V. Aishwarya, K. G. Sheela, “An improved sepic-based single switch buck-boost pfc converter fed brushless dc motor drive”, Materials Today: Proceedings, Vol. 24, 2020, pp. 1855-1864.